



Journal Homepage: - [www.journalijar.com](http://www.journalijar.com)  
**INTERNATIONAL JOURNAL OF  
 ADVANCED RESEARCH (IJAR)**

Article DOI: 10.21474/IJAR01/2197  
 DOI URL: <http://dx.doi.org/10.21474/IJAR01/2197>



### RESEARCH ARTICLE

#### INVESTIGATION ON THE USE OF THE CEMENT MORTAR CONTAINING BANANA FIBERS AS THERMAL INSULATOR IN BUILDING.

\*Sibiath O. G. Osseni<sup>1</sup>, Clement Ahouannou<sup>1</sup>, Emile A. Sanya<sup>1</sup> and Yves Jannot<sup>2,3</sup>.

1. Laboratory of Applied Energetics and Mechanics (LEMA), Polytechnic School of Abomey-Calavi / University of Abomey-Calavi, 01 BP. 2009 Cotonou (Benin).
2. University of Lorraine, LEMTA, UMR 7563, Vandœuvre-les-Nancy, F-54500, France.
3. CNRS, LEMTA, UMR 7563, Vandœuvre-les-Nancy, F-54500, France.

#### Manuscript Info

##### Manuscript History

Received: 27 September 2016  
 Final Accepted: 30 October 2016  
 Published: November 2016

##### Key words:-

Composite materials, banana fibers, cement mortar, thermal insulator, building.

#### Abstract

This paper dealt with the valorization of Benin natural resources through the development of new composite materials made of banana fibers-cement mortar which could be used as thermal insulator in building. The developed composites were formulated and made by substituting a mix of sand and cement, in mass fractions, with the banana trunk fibers previously washed with hot water and dried. Cement was dosed at 250 kg m<sup>-3</sup> of mortar and the ratio W/C was equal to 0.7 for the samples. The effected thermal tests by the hot plate method using two temperature measurements had shown a decreasing of the thermal effusivity and conductivity when the proportion of fibers increased. One had obtained the respective relative deviations of 25.54%, 56.09% and 65.68% between the thermal conductivity of the reference sample, which was equal to 1.14 W m<sup>-1</sup> K<sup>-1</sup>, and that of the composites. These results made the composites interesting thermal insulators in building with reduction of the normally used quantity of cement and sand and valorization of agricultural waste. The water absorption was also calculated for each sample.

Copy Right, IJAR, 2016., All rights reserved.

#### Introduction:-

World energy consumption is increasing and this growth affects all sectors, particularly the construction and reflects the need for more performance, power and comfort in the different uses of energy. This situation is not without environmental impacts due to significant emissions of the greenhouse gas effects. Thus, the new composite materials are developed to serve as natural or not thermal insulators, while maintaining an acceptable mechanical strength. We find in this class of materials, the concrete reinforced by the fibers often got from agricultural residues. The use of local materials in construction of buildings is one of the potential ways to support sustainable development in both urban and rural areas in developing countries (Mostafa et al., 2015).

Many research studies have developed this technology and its variants according to the chemical, thermal and mechanical aspects. The thermal conductivity and the mechanical strength are determined to know the insulation property of the material and to classify it in its appropriate use category. In general, these studies have shown that, the incorporation of the lightweight aggregate in composites results in a decreasing of the thermal conductivity

**Corresponding Author:- Sibiath O. G. Osseni.**

Address:- Laboratory of Applied Energetics and Mechanics (LEMA), Polytechnic School of Abomey-Calavi / University of Abomey-Calavi, 01 BP. 2009 Cotonou (Benin).

[(Meukam et al., 2004), (Benazzouk et al., 2006), (Sow et al., 2009), (Taoukil et al., 2011), (Belkarchouche et al., 2013)]. These studies have also shown the influence of the aggregates proportion on the insulating capacity of the composite materials, as well as the effect of the applied treatment before their use.

For composite materials development, a growing interest is also found in the plant fibers as reinforcements for their availability in terms of their quantity, their annual regularity and their no conflicting usage. Among the most used fibers include flax fibers, hemp, jute, cane, bamboo, raffia, cotton, kapoc, coconut, abaca, sisal, curauá, alfa, banana ..., the majority has been physico-chemically, morphologically, mechanically and thermally studied and characterized (Ardanuy, 2015).

Toledo (1999), Wang et al. (2007), Tung et al. (2012) and Mostafa et al. (2015) showed that the addition of the fibers (coconut, sisal, flax, and banana) significantly improves the mechanical properties of the cementitious composites, like flexural strength, Compressive strength, ductility, which can be used for the production of structural elements in building. Note that the fibers have previously undergone various treatments, in order to ensure the durability of the materials.

In this study, we have selected the banana trunk fibers as reinforcement element to the usual cement matrix because it is a renewable resource, locally available in Benin and there is a few works reported in the literature on composites made of cement mortar-banana trunk fibers. The overall objective is the valorization of Benin natural resources through the development of new composite materials banana fibers-cement mortar which can be used as thermal insulator in building. The thermal characterization will then allow us to assess the effect of fibers incorporation in the matrix mortar.

## Materials and methods:-

### Materials:-

#### Banana trunk:-

Banana plant is from the hot, humid tropical jungles of Southeast Asia. From the Musaceae family, banana would be the largest herbaceous flowering plant. Its trunk consists of a single branch which, towards the end of its life, will generate a regimen of fruits called "bananas". It has a buzzing rhizome that gives rise to leaves with sheaths. The stipe or pseudo-trunk has a large diameter up to 20 cm and a height, of up to 8 m, depending on the variety. The true stem of the banana plant does not exceed the ground level: the rhizome, from which are born (up) auxiliary buds that give discharges, ensuring the sustainability of the species and (down) of roots which penetrate into the ground (Fig 1).



**Fig 1:-** Picture showing a cut trunk of banana plant

The banana production continues, according to FAOSTAT in 2014, to grow both in Benin and in the rest of West Africa. A banana "tree" or plant often produces only one regimen of fruits at a time, hence the importance of the cut, after harvest, to make place for a next one. This raw material is then always locally available.

**Fibers extraction and processing:-**

The banana tree trunks are cut after collecting the banana stems and detached in scales. The fibers extraction is done manually using a dull knife which serves to scrape the scales surface. All fibers obtained are soaked in hot water and dried after cooling in order to remove surface impurities. They are also rinsed with tap water and dried at 60 °C five times to reduce their water absorption capacity. The fibers (Fig 2) are then cut at an average length of 30 mm using scissors.



**Fig 2:-** Picture showing the banana trunk fibers.

**Composites formulation:-**

The mortar samples consist of CPJ 35 cement giving a compressive strength at 28 days equal to 35 MPa, the lagoon sand with grains diameter less than 4 mm and the cement is dosed at 250 kg m<sup>-3</sup> of the mixture. The ratio W/C is equal to 0.7 to allow composites molding.

The weighed and pre-wetted fibers are thoroughly drained and added gradually to the mortar in the proportions of 1%, 2% and 3% by substitution to the equivalent percentages in mass of cement and sand mixture. Beyond 3%, we get a little malleable mixture and difficult to mold (Fig 3). All samples are molded into the dimensions: 10 × 10 × 3 cm<sup>3</sup> (Table 1, Fig 4). They are dried in the open air for 48 h, oven dried for 24 h at 103 °C ± 2°C then packed in zip bags for three days before testing. This set up condition allows homogenizing the moisture in the material.



**Fig 3:-** Picture showing the reinforced composite by 4% of banana trunk fibers.

**Table 1 :-** Samples characteristics

Samples	Fibers proportion F (%)	W/C	Dry samples weight (g)
Reference	0	0.7	600.8
Composite 1	1	0.7	518.6
Composite 2	2	0.7	460.7
Composite 3	3	0.7	405.8



**Fig 4:-** Picture of few samples used for thermal characterization.

#### **Methods:-**

##### **Determination of samples density:-**

The dry samples are weighed ( $M_{dry}$ ) on a digital scale with 0.1 g precision and their masses are related to their volumes ( $V$ ) calculated from the geometric dimensions taken using a digital caliper Facom of 0.05 mm precision. The density is calculated as:

$$\rho = \frac{M_{dry}}{V} \quad (1)$$

##### **Determination of the water absorption:-**

Operations are performed in the following order:

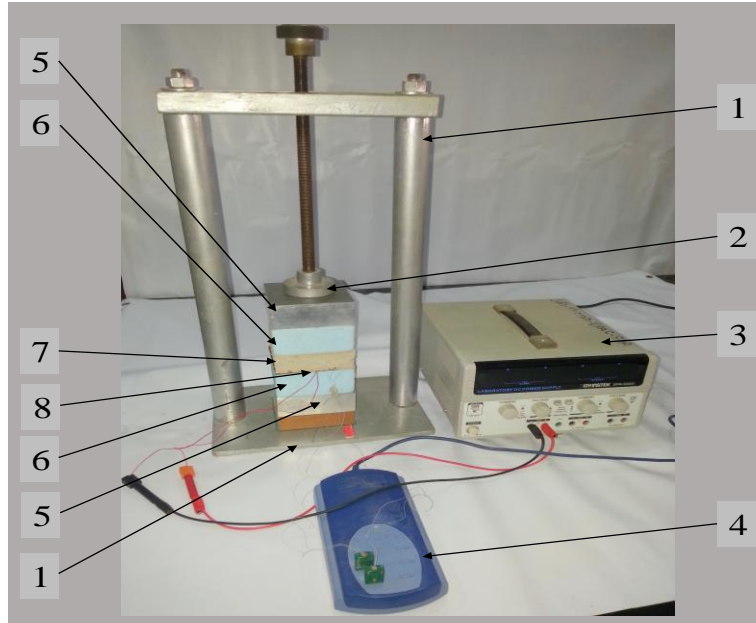
- ❖ immersion in a water tank at  $28 \pm 2$  ° C for 72 hours. Before weighing ( $M_{wet}$ ), the sample is wiped with a soft cloth to rid the superficial water
- ❖ drying for 72 h in a ventilated oven whose temperature is maintained at  $103 \pm 2$  ° C.

The weight is considered constant when two successive weighing 24 h do not give a greater than 0.1% difference. The water absorption ( $Abs$ ) is expressed in percent of the dry mass and is calculated by the following relationship:

$$Abs = \frac{M_{wet} - M_{dry}}{M_{dry}} \times 100. \quad (2)$$

##### **Thermal properties measurement:-**

The thermal properties, such as thermal effusivity, the volumetric heat capacity and thermal conductivity, are determined by the hot plate method with two temperature measurements (Figs 5 and 6).



1- Stem, 2- clamping device, 3- stabilized supply, 4- temperature recorder, 5- aluminum blocks, 6- insulators, 7- sample, 8- heating element

**Fig 5:-** Picture of the used asymmetric hot plate device.

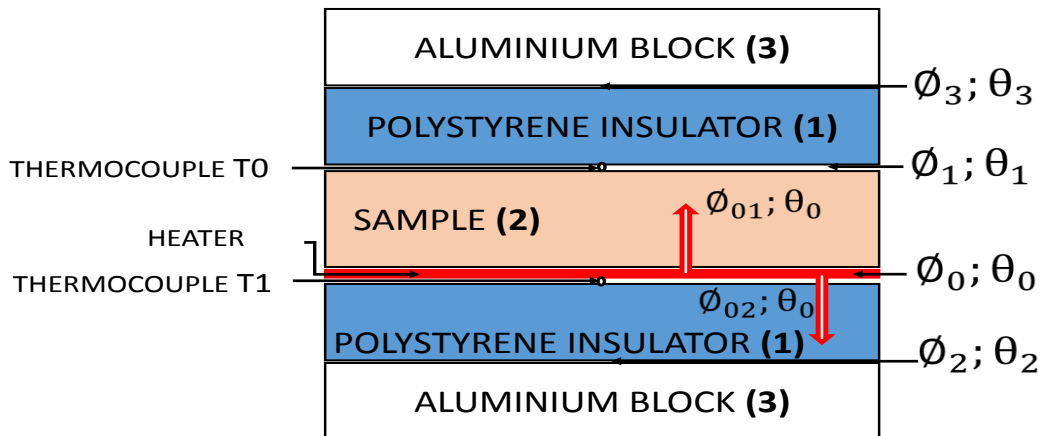


**Fig 6:-** Equivalent schema of the asymmetric hot plate device in insulated rear face mounting.

Fig 6 presents a schema of the device. A plane heat source is inserted between a polystyrene block (1) and a sample to be characterized (2). The upper face of sample (2) is in contact with a polystyrene sample. The outer faces of the two polystyrene blocks are maintained at ambient temperature by contact with massive aluminium blocks (3). The heat plate element has the following characteristics: Area:  $\approx 0.0103 \text{ m}^2$  ; thickness:  $e_h = 0.0003 \text{ m}$ ; electrical resistance:  $R_{el} = 41.3 \Omega$ . The thermal properties of the polystyrene blocks measured by Setaram  $\mu\text{dsc}3$  calorimeter and Netzsch HFM are:  $\lambda = 0.032 \text{ W m}^{-1} \text{ K}^{-1}$  and  $\rho c = 4.8 \times 10^4 \text{ J m}^{-3} \text{ K}^{-1}$  and their thickness are 50 mm.

The temperatures of the two aluminium blocks are equal and identical. A good thermal contact is achieved because the components of the hot plate (insulating blocks, aluminum blocks, heater and thermocouple) are correctly set on the tray of the gallows by a clamping device with a moderate holding pressure provided by a threaded metal pin.

Three-dimensional modeling of hot plate with two temperature measurements:-  
The transfer in the sample can be modeled in 3D as followed (Fig 7):

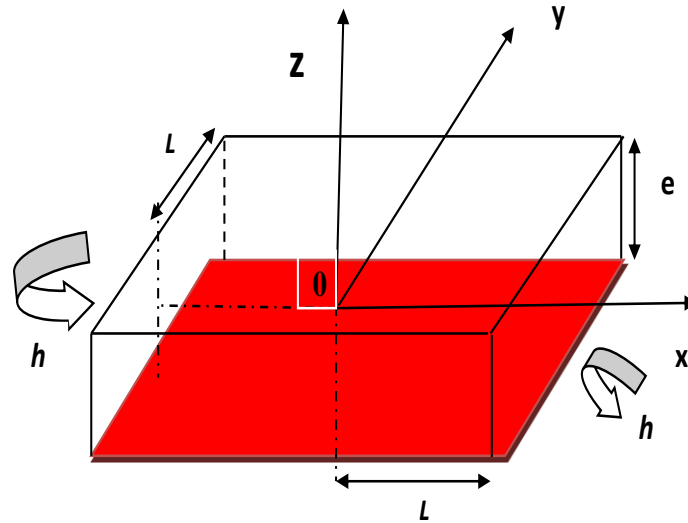


Fig 7:- A 3D modeling of transfers in the sample.

The heat equation is:-

$$\frac{\partial^2 T(x, y, z, t)}{\partial x^2} + \frac{\partial^2 T(x, y, z, t)}{\partial y^2} + \frac{\partial^2 T(x, y, z, t)}{\partial z^2} = \frac{1}{a} \frac{\partial T(x, y, z, t)}{\partial t} \tag{3}$$

The initial and boundary conditions are written:

at  $t = 0, T_0(x, y, z, 0) = T_{i0}, T_1(x, y, z, 0) = T_{i1}$

$$-\lambda \frac{\partial T(x, y, 0, t)}{\partial z} = \frac{T_{i0}(x, y, 0, t) - T_0(x, y, 0, t)}{R_{c1}} \tag{4}$$

$$-\lambda \frac{\partial T(x, y, e, t)}{\partial z} = \frac{T_{i1}(x, y, e, t) - T_1(x, y, e, t)}{R_{c2}} \tag{5}$$

$$\frac{\partial T(0, y, z, t)}{\partial x} = 0 \tag{6}$$

$$\frac{\partial T(x, y, z, t)}{\partial y} = 0 \tag{7}$$

$$-\lambda \frac{\partial T(x, L, z, t)}{\partial y} = h[T(x, L, z, t) - T_{i0}] \tag{8}$$

$$-\lambda \frac{\partial T(L, y, z, t)}{\partial x} = h[T(L, y, z, t) - T_{i0}] \tag{9}$$

$$\phi_0 = (\rho e c)_s \frac{\partial T_0(x, y, z, t)}{\partial t} + \frac{T_{i0}(x, y, 0, t) - T_0(x, y, 0, t)}{R_{c1}} \tag{10}$$

$a$  thermal diffusivity ( $\text{m}^2 \text{s}^{-1}$ );  $e$  thickness (m);  $R_c$  thermal contact resistance ( $\text{K W}^{-1}$ );  $h$  convection coefficient ( $\text{W m}^{-2}\text{K}^{-1}$ );  $\rho$  density ( $\text{kg m}^{-3}$ ).

The analytical solution of equation (3) with initial and boundary conditions, equations (4 to 10), by the variables separation method and the Laplace transform is complex. But the numerical method, based on Comsol simulations of the device and the quadrupole modeling, is the most used.

### Quadrupole modeling:-

Fig 6 defined the used notations in the model, as the Laplace transform of the temperature and the Laplace transform of the heat flux density, then the location of the two thermocouples in the experimental device. It is considered that the transverse dimensions of the heater is large compared to the sample thickness. The heat transfer is therefore unidirectional in the central area of the device.

The thermal contact resistances, at the interfaces of heating element/polystyrene and sample/polystyrene, have been neglected because of the contact with a soft and flexible thermal insulator. Considering that the heating element is enough thin such that we can apply the quadrupole formalism (Maillet, 2000) which gives:

$$\begin{bmatrix} \theta_0 \\ \phi_{01} \end{bmatrix} = \begin{bmatrix} 1 & 0 \\ mc_h p & 1 \end{bmatrix} \begin{bmatrix} 1 & R_c \\ 0 & 1 \end{bmatrix} \begin{bmatrix} A_s & B_s \\ C_s & D_s \end{bmatrix} \begin{bmatrix} A_i & B_i \\ C_i & D_i \end{bmatrix} \begin{bmatrix} 0 \\ \phi_3 \end{bmatrix}, \quad (11)$$

$$\begin{bmatrix} \theta_0 \\ \phi_{02} \end{bmatrix} = \begin{bmatrix} A_i & B_i \\ C_i & D_i \end{bmatrix} \begin{bmatrix} 0 \\ \phi_2 \end{bmatrix}, \quad (12)$$

with:  $A_s = D_s = ch(q_s e_s)$ ,  $B_s = \frac{1}{\lambda_s q_s} sh(q_s e_s)$ ,  $C_s = \lambda_s q_s sh(q_s e_s)$ ,  $q_s = \sqrt{\frac{p}{a_s}}$ ,

$A_i = D_i = ch(q_i e_i)$ ,  $B_i = \frac{1}{\lambda_i q_i} sh(q_i e_i)$ ,  $C_i = \lambda_i q_i sh(q_i e_i)$ ,  $q_i = \sqrt{\frac{p}{a_i}}$ ,

where:

$\theta_0$  Laplace transform of the temperature in the heated face;  $\phi_{01}$  Laplace transform of the heat flow density crossing the sample;  $\phi_{02}$  Laplace transform of the heat flow density crossing the bottom insulator;  $\phi_3$  Laplace transform of the heat flow density on the upper face of the top insulator;  $c$  specific heat ( $\text{J kg}^{-1} \text{K}^{-1}$ );  $p$  Laplace parameter ( $\text{s}^{-1}$ );  $m$  mass of the heating element (kg). The indices i and s mean respectively insulator and sample.

The equations (11) and (12) lead to:  $\phi_{01} = \theta_0 \frac{D_0}{B_0}$  and  $\phi_{02} = \theta_0 \frac{D_i}{B_i}$ ,

with:  $\phi_0 = \frac{\phi_0}{p} = \phi_{01} + \phi_{02}$ , where  $\phi_0 = \frac{Rel}{S} \times I^2$  is the heat flux density produced by Joule effect in the heating element.

Setting:

$$\begin{bmatrix} A_0 & B_0 \\ C_0 & D_0 \end{bmatrix} = \begin{bmatrix} 1 & 0 \\ mc_h p & 1 \end{bmatrix} \begin{bmatrix} 1 & R_c \\ 0 & 1 \end{bmatrix} \begin{bmatrix} A_s & B_s \\ C_s & D_s \end{bmatrix} \begin{bmatrix} A_i & B_i \\ C_i & D_i \end{bmatrix}$$

Then:

$$\theta_0 = \frac{\phi_0}{\left(\frac{D_i + D_0}{B_i + B_0}\right)}, \quad (13)$$

The thermal balance between the heater and the unheated face of the sample can be written

$$\begin{bmatrix} \theta_0 \\ \phi_{01} \end{bmatrix} = \begin{bmatrix} 1 & 0 \\ mc_h p & 1 \end{bmatrix} \begin{bmatrix} 1 & R_c \\ 0 & 1 \end{bmatrix} \begin{bmatrix} A_s & B_s \\ C_s & D_s \end{bmatrix} \begin{bmatrix} \theta_1 \\ \phi_1 \end{bmatrix}, \quad (14)$$

where:

$\theta_1$  Laplace transform of the temperature in the unheated face;  $\phi_1$  Laplace transform of the heat flow density on the unheated face of the sample

setting:

$$\begin{bmatrix} A_2 & B_2 \\ C_2 & D_2 \end{bmatrix} = \begin{bmatrix} 1 & 0 \\ mc_h p & 1 \end{bmatrix} \begin{bmatrix} 1 & R_c \\ 0 & 1 \end{bmatrix} \begin{bmatrix} A_s & B_s \\ C_s & D_s \end{bmatrix},$$

Then:

$$\theta_1 = \theta_0 \left( D_2 - \frac{D_0}{B_0} B_2 \right). \quad (15)$$

The temperatures  $\theta_0$  and  $\theta_1$  in equations (13) and (15) are obtained in the Laplace space. The inverse Laplace transformation is realized by using the De Hoog algorithm (De Hoog, 1982) to calculate the temperature of the heated face  $T_0$  and the temperature of the unheated face  $T_1$ .

The principle of this method consists to estimate the value of the parameters  $E_s$  and  $\rho_s c_s$ , which is the product of the density ( $\text{kg m}^{-3}$ ) and the specific heat, of the sample that minimize the sum of the quadratic error  $\Psi = \sum_{i=1}^N [T_{exp}(t_i) - T_{mod}(t_i)]^2$  between the experimental and the theoretical temperature curves calculated from equations (13) and (15).

**Estimation method of the thermal parameters:-**

The estimation errors on the two thermal parameters of the samples to be characterized are due to the uncertainties on the "known parameters", the noise on the temperature measurements and an error model when a 1D model is used to represent a 3D heat transfer.

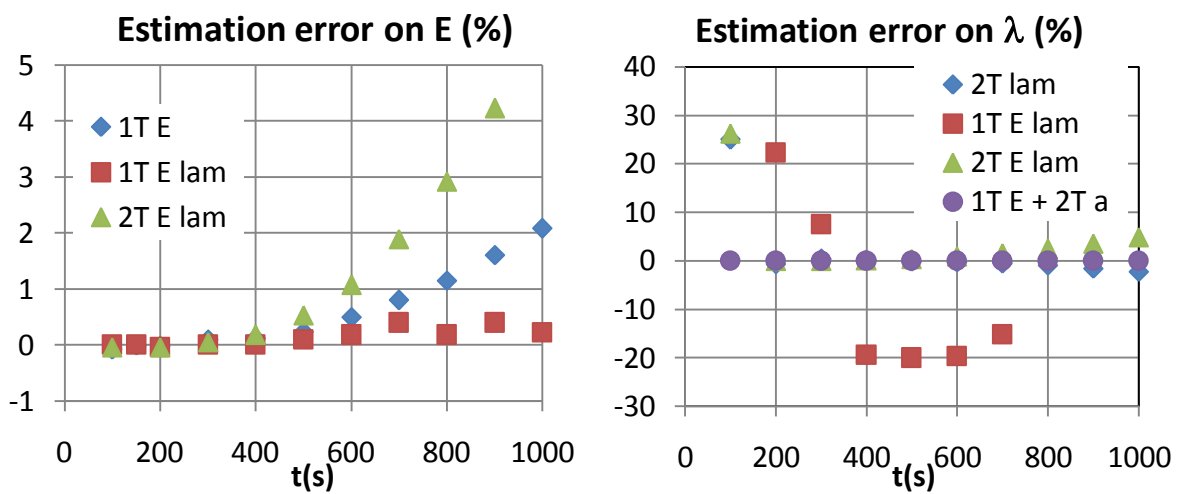
The following method has been used to evaluate the two last estimation errors as a function of time interval, for one surface temperature measurement method on one hand, and for two surfaces temperature measurement method on the other, considering two structure materials, respectively: a) cellular concrete (low density and conductivity) and b) concrete (high density and conductivity) which thermal properties are: (Taine et al., 2014)

Cellular concrete:  $e = 3 \text{ cm}$ ;  $\lambda = 0.16 \text{ W m}^{-1} \text{ K}^{-1}$ ;  $\rho c = 3.3 \times 10^5 \text{ J m}^{-3} \text{ K}^{-1}$

Concrete:  $e = 3 \text{ cm}$ ;  $\lambda = 1.75 \text{ W m}^{-1} \text{ K}^{-1}$ ;  $\rho c = 2.2 \times 10^6 \text{ J m}^{-3} \text{ K}^{-1}$

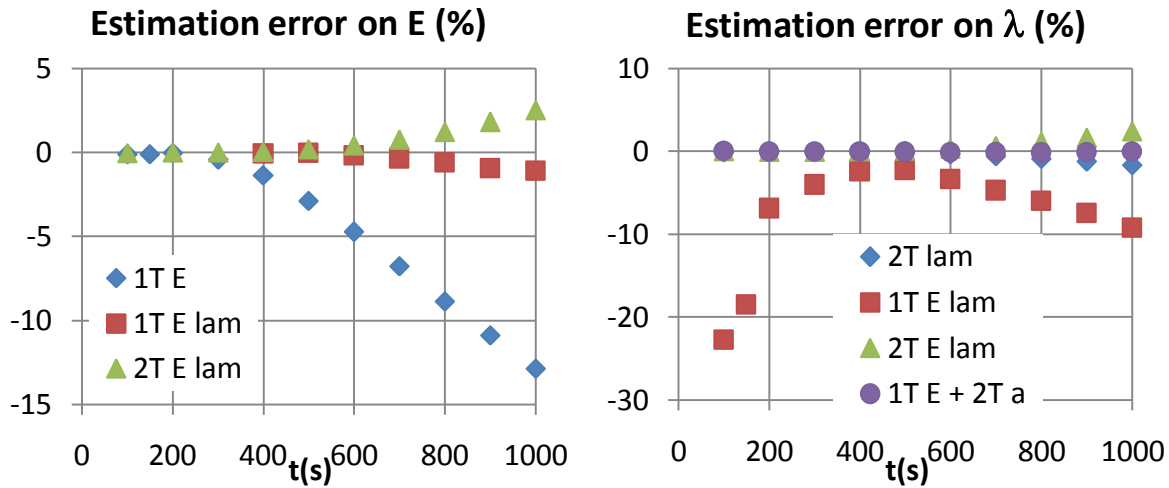
- ❖ a 3D simulation of  $T_0$  and  $T_1$  is realized using COMSOL software and considering a constant time step of 0.1 s
- ❖ a random noise with a standard deviation value  $\sigma T = 0.1 \text{ }^\circ\text{C}$  is added to each signal
- ❖ these simulated and noised curves  $T_0(t)$  and  $T_1(t)$  are used as experimental curves to estimate the thermal parameters by three different methods :
- ❖ the relative deviations of the estimated values from the initial values used in COMSOL simulations are calculated.

The best estimation method will be the one which gives the lower relative error. Fig 8 shows that the best method to estimate  $E_s$  is the "1T E lam" method enabling a precise estimation on the larger time interval. Then, the best way to estimate the other parameters is to estimate the thermal diffusivity  $a_s$  by the "1T E + 2T a" method enabling a precise estimation of  $a_s$  until 800 s. The other parameters  $\rho_s c_s$  and  $\lambda_s$  can then be calculated from the determined values of  $E_s$  and  $a_s$ .



a) For cellular concrete





b) For concrete

**Fig 8:-** Relative errors for the thermal parameters estimated by three different methods : estimation of  $E_s$  using  $T_0$  (“1T E”), estimation of  $E_s$  and  $\lambda_s$  using  $T_0$  (“1T E lam”), estimation of  $E_s$  and  $\lambda_s$  using  $T_0$  and  $T_1$  (“2T E lam”), estimation of  $a_s$  using  $T_0$  and  $T_1$  with  $E_s$  known by “1T E” method (“1T E + 2T a”).

**Results and Discussions:-**

After calibrating the device, the estimated surface of the heating element was  $0.0105 \text{ m}^2$  and its estimated thermal capacity was  $428.6 \text{ (J K}^{-1}\text{)}$ . From the different measurements, we plotted the graphs of the figures 9 to 12.

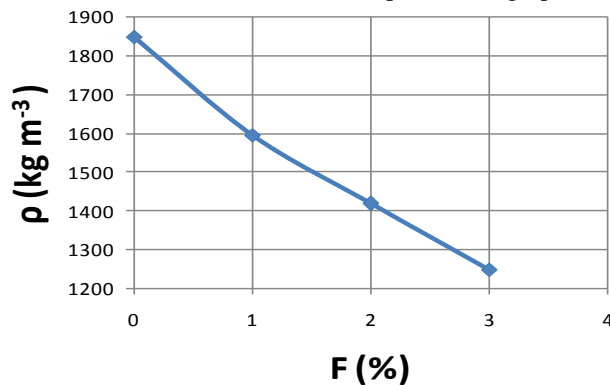


**Fig 9:-** Density of the samples as a function the fibers mass fractions (F).

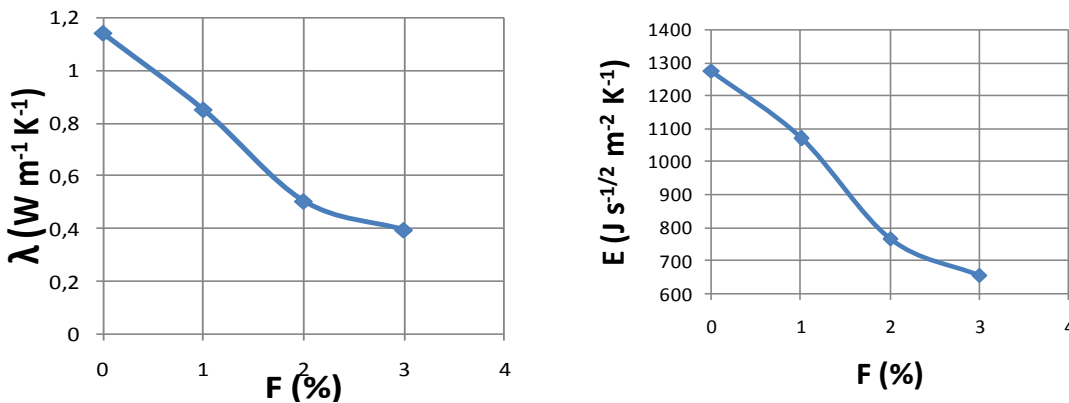


**Fig 10:-** Thermal conductivity and effusivity as the functions of fibers mass fractions (F).

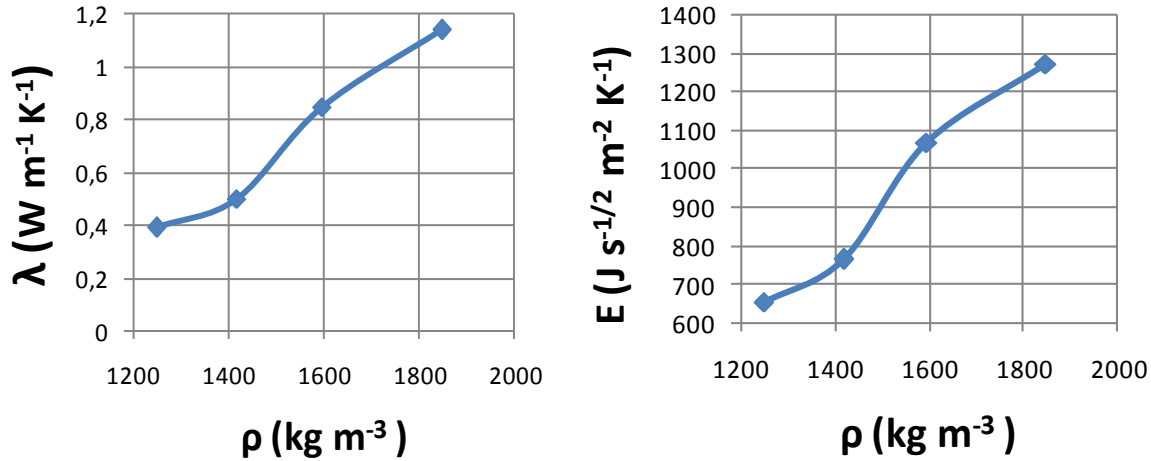


Fig 11:- Thermal conductivity and effusivity as the functions of the density.

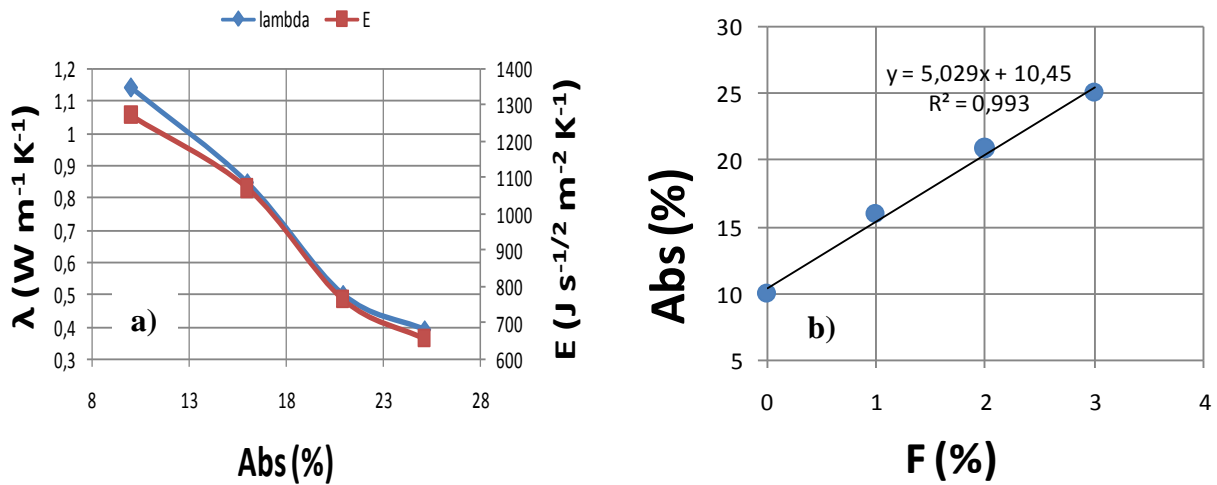


Fig 12:- a) Thermal effusivity and conductivity as function of water absorption; b) Water absorption as function of fibers mass fractions.

**Density and thermal properties:-**

It could be noted that the density, the thermal effusivity and the thermal conductivity decreased when the percentage of incorporated fibers increased, giving respective relative deviations of 25.54%, 56.09% and 65.68% between the thermal conductivity of the reference sample, which was equal to 1.14 W m<sup>-1</sup> K<sup>-1</sup>, and that of the composites. An analysis of the results on these figures allowed concluding that the cement mortars containing banana trunk fibers were more insulating than conventional mortar.

**Water absorption:-**

Fig. 12 showed that the water absorption was substantially linear and increased respectively of about 1.5, 2 and 2.5 times for composites containing 1%, 2% and 3% of fibers in relation to the reference. Similarly, the thermal effusivity and conductivity decreased when the absorption rate increases. Depending on the climate, these composites would be used alone in construction or set in sandwich with a less hygroscopic and insulating material to reduce their ability to absorb water for example and to guarantee their durability.

These results were interesting because in a tropical climate, low heat conductivity materials and low specific heat were searched for thermal insulation in building. These materials could be used, for example, to fill a carrier structure, to achieve the insulating boards, for cladding or for internal partitions valuing agricultural waste while reducing the quantities of used cement and sand.

**Conclusion:-**

One have formulated and made composites containing banana trunk fibers previously washed with hot water and dried. Cement were dosed at  $250 \text{ kg m}^{-3}$  of mortar with a ratio  $W / C$  equal to 0.7. By using the hot plate method, one had shown a strong relationship between the fibers proportion and the thermal effusivity and conductivity for new synthesized composite materials. Then, these properties made to these materials, the candidates for thermal insulators in building. The water absorption was also function of the fibers proportion. A further study on mechanical properties and microstructure of the fibers and the composites would allow defining their optimal use conditions.

**References:-**

1. Marwan Mostafa and Nasim Uddin (2015): Effect of Banana Fibers on the Compressive and Flexural Strength of Compressed Earth Blocks. *Build.*, 5: 282-296.
2. Meukam P., Jannot Y., Noumowe A. and Kofane T. C. (2004): Thermo physical characteristics of economical building materials. *Constr. Build. Mater.*, 18: 437-443.
3. Benazzouk A., Douzane O., Mezreb K., Laidoudi B., Queneudec M. (2006): Thermal conductivity of cement composites containing rubber waste particles: experimental study and modeling. *Constr. Build. Mater.*, 22: 573-579.
4. Sow D., Gaye S., Adj M. and Azilidon D. (2009): Valorization of Agricultural Wastes by their Integration in Construction Materials: Application to Rice Straw, paper presented at AMSE International Conference MS'09, Trivandrum, India.
5. Taoukil D., EL Bouardi A., Ajzoul T., Ezbakhe H. (2011): Caractérisation mécanique et hydrique d'un béton allégé avec les résidus de bois. *Revue internationale d'héliotechnique*, 43 : 1-7.
6. Belkarchouche D., Chaker A. (2013): Caractérisation thermophysique et mécanique de matériaux de construction: béton de fibre naturelle, paper presented at JITH, Marrakech, Maroc.
7. Mônica Ardanuy, Josep Claramunt, Romildo Dias Toledo Filho (2015): Cellulosic fiber reinforced cement-based composites: A review of recent research. *Constr. Build. Mater.*, 79: 115–128.
8. Romildo Dias Tolêdo Filho, Kuruvilla Joseph, Khosrow Ghavami, George Leslie England (1999): The use of sisal fibre as reinforcement in cement based composites. *Rev. Bras. Eng. Agr. Amb.*, 3: 245-256.
9. Li Zhijian, Wang Lijing and Wang Xungai (2007): Cement composites reinforced with surface modified coir fibers, *Journal of composite materials. J. Comp. Mater.*, 41: 1445-1457.
10. Tung L. H., Khadraoui F., Boutouil M., Gomina M. (2012) Analyse microstructurale et mécanique d'un composite cimentaire renforcé par des fibres de lin, paper presented at 20<sup>th</sup> University Meetings of Civil engineering, Chambéry.
11. Maillet D., Andre A., Batsale J.C., Degiovanni A., Moyne C. (2000): *Thermal quadrupoles* (John Wiley & Sons Ltd).
12. De Hoog FR. (1982): An improved method for numerical inversion of Laplace transforms. *Soc. Ind. Appl. Math.*, 3(3): 357–366.
13. Taine J., Enguehard F., Iacona E. (2014): *Transferts thermiques* (5th edition, Dunod, Paris).

**List of reviewers:-**

1. Gaye Salif , University Cheikh Anta Diop / Senegal
2. Chaker Abla, University of Constantine 1 / Algeria
3. Michèle Quéneudec, University of Picardie Jules Verne / France